

# Nanosecond Pulsed Power Generator for a Voltage Amplitude up to 300 kV and a Repetition Rate up to 16 Hz for Fine Disintegration of Quartz

E. G. Krastelev\*, A. A. Sedin, and V. I. Tugushev

*Joint Institute for High Temperatures, Russian Academy of Sciences,  
ul. Izhorskaya 13, str. 2, Moscow, 125412 Russia*

\*e-mail: ekrastelev@yandex.ru

Received February 25, 2015

**Abstract**—A generator of high-power high-voltage nanosecond pulses is intended for electrical discharge disintegration of mineral quartz and other nonconducting minerals. It includes a 320 kV Marx pulsed voltage generator, a high-voltage glycerin-insulated coaxial peaking capacitor, and an output gas spark switch followed by a load, an electric discharge disintegration chamber. The main parameters of the generator are as follows: a voltage pulse amplitude of up to 300 kV, an output impedance of  $\approx 10 \Omega$ , a discharge current amplitude of up to 25 kA for a half-period of 80–90 ns, and a pulse repetition rate of up to 16 Hz.

**Keywords:** pulsed voltage generator, coaxial transmission line, spark switch, selective fragmentation.

**DOI:** 10.1134/S1063778815140082

Electrical-discharge selective disintegration of mineral quartz attracts more and more attention in relation to the possibility of obtaining high quality products in an ecologically clean way. One of the key tasks in solving this problem is the creation of high-power high-voltage pulses with the parameters satisfying the requirements of electric discharge technologies whose resource is sufficiently large for providing long-term operation with a pulse repetition rate of up to 10–20 Hz.

Studies on creation of generators are performed along several lines including the improvement of conventional technology of pulsed voltage Marx generators [1, 2] and the development of designs with a high-voltage pulsed transformer [3].

Below, we describe the design of a generator based on the use of a pulsed voltage generator (PVG) supplemented with a coaxial peaking capacitor with an output switching gap and a connected discharge chamber. Such a generator design provides a high rate of voltage buildup in the gap and its maintenance during the breakdown delay time, increases the efficiency of energy input to the discharge channel owing to low internal resistance and short coaxial capacitor discharge time, and provides a safe operating mode of the PVG capacitors. The use of glycerin as an insulation of the peaking capacitor makes it possible to design it as a compact maintenance-free structure.

## GENERATOR STRUCTURE AND DESIGN

*Pulsed voltage generator.* The PVG design implies bipolar charging. It includes four cascades each of which includes two 20 nF KPCh-50-0.02 capacitors charged to a voltage of +40 kV and –40 kV with a rated lifetime of  $5 \cdot 10^8$  charging–discharging cycles for a nominal charging voltage of 50 kV and a reverse voltage of not more than 10%. The total accumulated energy is 128 J, the shock voltage is 320 kV, and the “shock” capacity is 2.5 nF.

The pulsed voltage generator has resistive cascade interconnections. The calculation of thermal losses in the charging–discharging cycle resulted in choosing 4 k $\Omega$  resistors.

The PVG is mounted in a tank with a cross section of  $74 \times 107 \text{ cm}^2$  and a height of 60 cm filled with transformer oil as an electric insulator.

*The charging device* is designed as a separate unit based on a ZNOM-35-65U1 transformer with a capacitive current limiting in the high-voltage line and a bipolar rectifier in the PVG tank; the rectifier is based on two SDL-0.4-1600 diode assemblies used to charge capacitors of positive and negative PVG parts in turn during several half-waves of the line voltage. If three KPCh-50-0.02 capacitors connected in parallel are

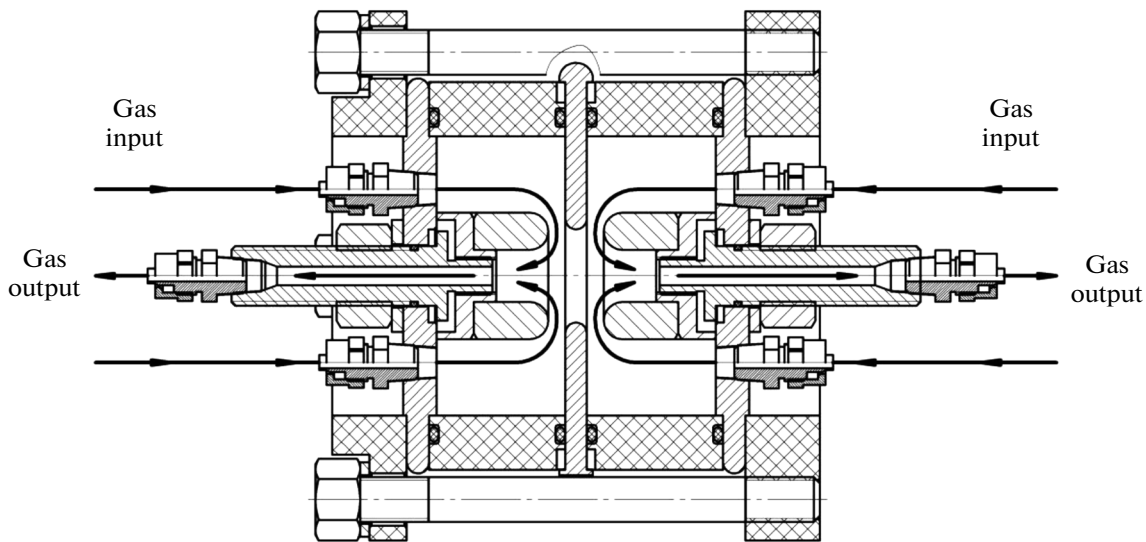


Fig. 1. Design of PVG gas spark switches.

used as a current limiting capacity, the PVG charging time is  $\approx 50$  ms.

*Switching discharge chambers of PVG.* Durable stable PVG operation is provided by gas spark switches with preionization by an additional corona discharge and gas (dried air, nitrogen) blow-through at a pressure of up to 3 atm. The design of the gas spark switches is shown in Fig. 1. This figure also shows the schematic diagram of the gas flow through the spark switches.

The spark switches have three electrodes; the control electrode is shaped as a disk with a hole in the middle of the interval between the two main electrodes. These spark switches differ from similar ones with “field distortion” with a thin disk used in PVG in the mode of single pulses in application of a thick (6 mm) disk for efficient heat removal and longer lifetime.

For the thicker middle electrode, there is no region of a highly inhomogeneous field near the hole edge (“field distortion” effect) when its potential changes under the impact of the initiating pulse. Poorer dynamic characteristics connected with this fact, in particular, larger breakdown delay time, is compensated by the preliminary gas ionization in the spark gaps using an additional corona discharge. According to the schematic diagram proposed in [4], the main electrodes have a toroidal working surface, and the additional corona-forming electrode is installed in the cavity of one of these electrodes. The outer diameter of the toroidal electrodes is 34 mm, the inner diameter is 16 mm, and the gap between the top of the main electrode and the control disk is 8.5 mm. The working parts of the electrodes are manufactured from an erosion-resistant copper–tungsten (70%W–30%Cu) composite material.

The working gas is fed into the spark switch through the fittings in the edge flanges along the surface of the insulation casing. After passing the discharge region, the heated and partly ionized gas is output through the cavities of the main electrodes and axial channels in the electrode holders. This blowing layout prevents electrode erosion products from depositing on the surface of the insulation casing and provides gas cooling and deionization as it flows in extended output channels.

*The PVG is initiated* by feeding pulses with an amplitude of about 60 kV to the control electrodes of the first two discharge chambers from the output of the pulsed transformer of the “initiation” generator whose schematic diagram and design are considered in [5].

*Peaking capacitor.* The peaking capacitor is made as a part of a coaxial line with glycerin insulation ( $\epsilon \approx 44$ ). The outer electrode diameter is 300 mm, the inner electrode diameter is 168 mm, and the line length is 580 mm. For this size, the capacitance with allowance for the edges and the lead-in line is approximately equal to the PVG “shock” capacity.

The design of the capacitor, the output switching discharge chamber, and the disintegration chamber above it is shown in Fig. 2.

The capacitor is placed vertically on the upward flange of the coaxial T-branch at the PVG output. The Plexiglas insulation diaphragms separate the glycerin-insulated line from the transformer-oil-filled volume of the lead-in line (T-branch) and gas insulation of the spark switch. For reducing the discharging rate, an additional inductance coil is installed between the PVG and the capacitor.

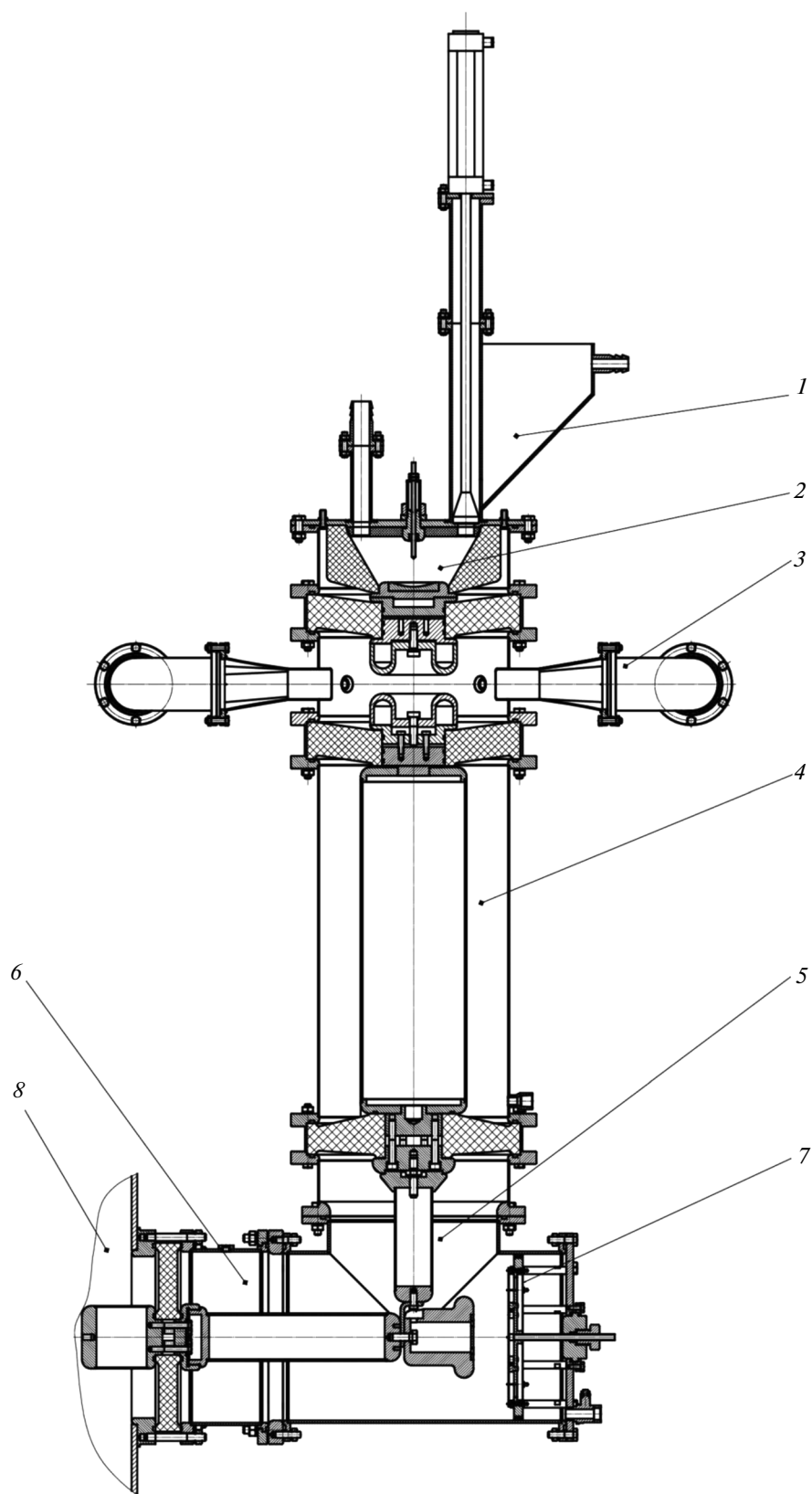


**Fig. 2.** Design of peaking capacitor with output gas spark switch and installed disintegration chamber. (1) Feeding bin, (2) disintegration chamber, (3) gas spark switch blow-through channel, (4) glycerin-insulated coaxial line, (5, 6) oil-insulated charging lines, (7) capacitance divider, and (8) PVG.

The output gas spark switch is a two-electrode, uncontrollable one. The working gas is dried air or nitrogen with an excess pressure of up to 3 atm. The spark switch is blown via a closed path with partial gas exchange (15–20 L/min) for preventing accumulation of electrode erosion products. High operation stability of the spark switch with a repetition rate of up to 16 Hz is achieved by gas preionization in the spark gap between the pulsed corona discharge ignited by a pointed electrode installed in the cavity of one of the main toroidal electrodes. The geometry of the spark and corona gaps are similar to those considered in [4], except that the size corresponds to a much higher voltage for the same scheme. The measured spread of the breakdown voltage for fixed working parameters does not exceed 3%.

**Disintegration chamber.** The layout of an “inverted” gap with grounded pin electrode is chosen for the electrical discharge chamber; this layout most naturally agrees with the output of the vertical coaxial line.

The chamber is formed by a cup-shaped insulator; a high-voltage electrode with a plane or spherical part of the working surface and a switching pin electrode at the upper grounded flange is attached to the bottom of this insulator. The pin electrode is shaped as a stud bolt, which makes it possible to control the working gap without opening the chamber.

The material is disintegrated batchwise, 1–1.5 kg each batch. The disintegration cycle lasts from 1 to 3 min depending on the required fractional composition (100–300  $\mu\text{m}$ ). The ready product is discharged through an output branch by a pulsed water flow supplied to the chamber via a separate input.

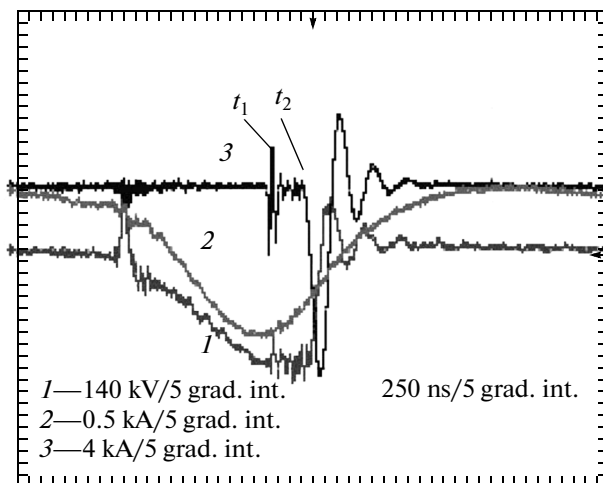


**Fig. 3.** (1) Voltage and (2) current curves at the PVG output and (3) discharge current in disintegration chamber.

## PERFORMANCE CHARACTERISTICS

The inductance and characteristic impedance of the discharge line calculated using the measured current oscillation period at short circuit in the disintegration chamber are  $\approx 250$  nH and  $\approx 10$   $\Omega$ , respectively. The current amplitude in the short-circuit mode is  $\approx 25$  kA for the discharge chamber breakdown at the maximum capacitor voltage.

Figure 3 shows the curves of voltage pulses at the PVG output, the PVG current, and the discharge current in the chamber in the operating mode during quartz disintegration.

When the threshold voltage is reached during the charging of the peaking capacitor at time instant  $t_1$ , the breakdown takes place in the output gas spark switch. The slight voltage drop and current oscillations observed after the breakdown are determined by the chamber capacity charging. As a result of continued charging of the peaking capacitor, the voltage on the capacitor and the chamber gap increase, reaching the maximum at time instant  $t_2$ , when the breakdown in the chamber takes place and the discharge current is observed to grow rapidly. In this case, the breakdown time delay is  $\approx 180$  ns. The duration of the first half-wave of the discharge current pulse is about 85 ns, and the buildup time is  $\approx 60$  ns.

The time instant of the output discharge initiation is chosen by adjusting the voltage from the condition of breakdown in the chamber near the maximum voltage on the peaking capacitor. In this case, at the time of discharge, most of the energy originally stored in the PVG is concentrated in the peaking capacitor. During its discharge, the fraction of energy passed back to the PVG is much smaller than that released in the plasma channel of the discharge. Low reverse voltage and the discharge current of PVG capacitors limited by additional charging inductance provide a safe operating mode.

## CONCLUSIONS

The created generator has been used for several years as a laboratory installation for fine disintegration of mineral quartz and other nonconducting materials. The experience of its operation demonstrated that the glycerin-insulated peaking capacitor stably operates in a periodic mode with a pulse repetition rate of up to 16 Hz, including in the presence of discharge current oscillations, without noticeable parameter variation and does not require any attendance. Low output resistance of the generator and nanosecond discharge

current pulse duration increase the energy efficiency of electrical-discharge fragmentation, making it competitive with conventional mechanical methods.

#### REFERENCES

1. H. Bluhm, W. Frey, H. Giese, P. Hoppe, C. Schultheib, and R. Strabner, *IEEE Trans. Dielectr. Electr. Insulat.* **7**, 625 (2000).
2. J. Hammon, D. Hopwood, M. Ingram, M. Klatt, and T. Tatman, in *Proceedings of the IEEE International Pulsed Power Conference, 2002*, p. 1142.
3. B. M. Kovalchuk, A. V. Kharlov, V. A. Vizir, V. V. Kum-pyak, V. B. Zorin, and V. N. Kiselev, *Rev. Sci. Instrum.* **81**, 103506 (2010).
4. E. G. Krastelev, in *Proceedings of the Scientific Session of Moscow Engineering Physics Institute MPhI-2006* (Moscow, 2006), Vol. 8, p. 45 [in Russian].
5. M. N. Baulin and E. G. Krastelev, in *Proceedings of the Scientific Session of Moscow Engineering Physics Institute MPhI-2009* (Moscow, 2009), Vol. 2, p. 161 [in Russian].

*Translated by E. Baldina*